AD-A133 513 DETERMINATION OF IONIZATION RATES IN THE PRINCIPAL CRYSTALLOGRAPHIC DIREC..(U) CORNELL UNIV ITHACA NY SCHOOL OF ELECTRICAL ENGINEERING C A LEE AUG 83 1/1

UNCLASSIFIED RADC-TR-83-182 F19628-79-C-0105 F/G 20/12 NL

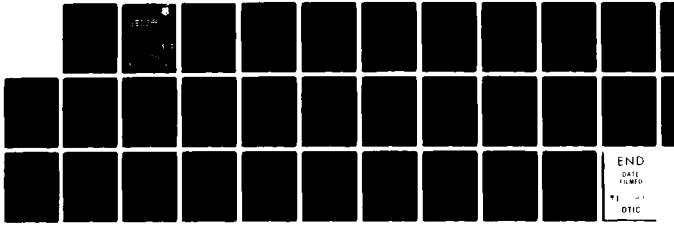

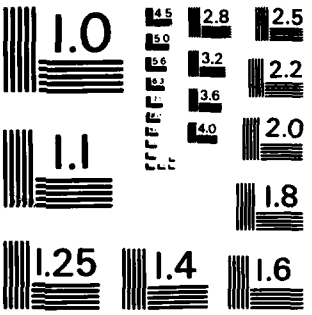

RADC-TR-83-182
Final Technical Report
August 1983

DETERMINATION OF IONIZATION RATES IN THE PRINCIPAL CRYSTALLOGRAPHIC DIRECTIONS IN SILICON

Cornell University

Charles A. Lee

ROME AIR DEVELOPMENT CENTER
Air Force Systems Command
Griffiss Air Force Base, NY 13441

This report has been reviewed by the RADC Public Affairs Office (PA) and is releasable to the National Technical Information Service (NTIS). At NTIS it will be releasable to the general public, including foreign nations.

RADC-TR-83-182 has been reviewed and is approved for publication.

APPROVED: J. P. Lorenzo

JOSEPH P. LORENZO
Project Engineer

APPROVED: Harold Roth

HAROLD ROTH, Director
Solid State Sciences Division

FOR THE COMMANDER: John P. Huss

JOHN P. HUSS
Acting Chief, Plans Office

If your address has changed or if you wish to be removed from the RADC mailing list, or if the addressee is no longer employed by your organization, please notify RADC (ESO) Hanscom AFB MA 01731 · This will assist us in maintaining a current mailing list.

Do not return copies of this report unless contractual obligations or notices on a specific document requires that it be returned.

UNCLASSIFIED

SECURITY CLASSIFICATION OF THIS PAGE (When Data Entered)

REPORT DOCUMENTATION PAGE		READ INSTRUCTIONS BEFORE COMPLETING FORM
1. REPORT NUMBER RADC-TR-83-182	2. GOVT ACCESSION NO. AD-A133513	3. RECIPIENT'S CATALOG NUMBER
4. TITLE (and Subtitle) DETERMINATION OF IONIZATION RATES IN THE PRINCIPAL CRYSTALLOGRAPHIC DIRECTIONS IN SILICON		5. TYPE OF REPORT & PERIOD COVERED Final Technical Report 1 May 79 - 30 Apr 81
		6. PERFORMING ORG. REPORT NUMBER N/A
7. AUTHOR(s) Charles A. Lee		8. CONTRACT OR GRANT NUMBER(s) F19628-79-C-0105
9. PERFORMING ORGANIZATION NAME AND ADDRESS Cornell University School of Electrical Engineering Ithaca NY 14853		10. PROGRAM ELEMENT, PROJECT, TASK AREA & WORK UNIT NUMBERS 61102F 2306J233
11. CONTROLLING OFFICE NAME AND ADDRESS Rome Air Development Center (ESO) Hanscom AFB MA 01731		12. REPORT DATE August 1983
		13. NUMBER OF PAGES 40
14. MONITORING AGENCY NAME & ADDRESS(if different from Controlling Office) Same		15. SECURITY CLASS. (of this report) UNCLASSIFIED
		15a. DECLASSIFICATION/DOWNGRADING SCHEDULE N/A

16. DISTRIBUTION STATEMENT (of this Report)

Approved for public release; distribution unlimited

17. DISTRIBUTION STATEMENT (of the abstract entered in Block 20, if different from Report)

Same

18. SUPPLEMENTARY NOTES

RADC Project Engineer: Joseph P. Lorenzo (ESO)

19. KEY WORDS (Continue on reverse side if necessary and identify by block number)

Silicon Junction Avalanche
Ionization Rates
Orientation Dependence
Photomultiplying detector
Threshold Ionization Energy
(Orientation Dependence)

20. ABSTRACT (Continue on reverse side if necessary and identify by block number)

Measurements of the electron and hole multiplication in silicon p-n junctions and the associated electron and hole ionization rates are presented for the three principal directions <100>, <110>, and <111>. It is shown that published ionization threshold energies are inconsistent with the experimental data. The inconsistency is traced to the fact that the appropriate non-colinear wave vector constructions for conserving crystal momentum in the ionizing collision process were not considered

DD FORM 1 JAN 73 1473 EDITION OF 1 NOV 65 IS OBSOLETE

UNCLASSIFIED

SECURITY CLASSIFICATION OF THIS PAGE (When Data Entered)

in the previous threshold calculations. An approximate solution to collisions with non-colinear wave vectors is presented that shows qualitative agreement with the experimental observations.

PREFACE

This report describes measurements of the ionization rates of electrons and holes in silicon pn junctions for the three principal crystalline directions ⟨100⟩, ⟨110⟩, ⟨111⟩. The work was conducted by Faculty and graduate students of the School of Electrical Engineering of Cornell University, Ithaca, New York under contract F19628-79-C-0105, and administered by the Electronics Systems Division, Hanscom Air Force Base, Massachusetts.

The work reported herein was performed during the period 5/1/79 to 4/30/81, the contract period, and the following two years by Prof. Charles A. Lee with a partial contribution by Bruce Shapiro, who left the project at an early stage. The contract was supervised by Dr. J. P. Lorenzo, Deputy for Electronic Technology at Hanscom AFB.

TABLE OF CONTENTS

LIST OF ILLUSTRATIONS

LIST OF TABLES

SECTION I
INTRODUCTION AND SUMMARY

The motivation for the present investigation was to see if reorienting the crystal direction of silicon photomultiplying detectors could lead to a reduction in their noise at high gain. The mean square current fluctuations in such detectors is proportional to the gain squared as long as the gain is less than the ionization rate ratio. If the gain exceeds the ionization rate ratio then the noise increases to something like the third power of the gain. Of all the semiconductors investigated so far, silicon has the highest ionization rate ratio, ranging from five to one hundred depending on the value of the electric field in the avalanche region.

Calculations of the threshold energies in various crystal directions had been published by Anderson and Crowell[1] showing nearly equal thresholds of about 3 eV for both electrons and holes for the ⟨111⟩ direction. This is the direction for which the high ionization rate ratio is observed.[2] Further, their calculations showed that in the ⟨100⟩ direction the threshold voltage for holes could be twice that (2 to 1 eV) of the electrons. In the ⟨110⟩ direction the ionization thresholds were about the same at approximately 2 eV, so presumably, the rates in this direction would be similar to the ratio found in the ⟨111⟩ direction.

The results of the measurements reported here, contrary to expectations, show the highest rates and the smallest ratio of rates is obtained in the ⟨100⟩ crystal direction, a slightly larger ratio is obtained in the ⟨110⟩ direction, and the largest ratio is obtained in the ⟨111⟩ direction. Since a careful rechecking of the measurements yielded the same result, some thought has been given to the threshold

calculations. In Anderson and Crowell's work only colinear momentum constructions of the initial and final particles through the zone center (i.e. k=0) were considered. During the course of this work colinear momentum constructions going through the conduction band minima and not through the zone center were considered. Neither of these sets of constructions corresponds to the observed ionization rates. Non-colinear constructions have been considered here in which the final particle velocities are colinear, but the wave vector from the Brillouin zone center to the conduction band minimum and the initial wave vector need not be colinear with the final velocities. This non-colinear problem is much more complex and is not solved in this report, but an approximation of it is presented that qualitatively agrees with the observed orientation dependence.

SECTION II
DESCRIPTION OF EXPERIMENT

1. Sample Preparation

A p-type boule of silicon was oriented and wafers were cut in the three principal crystallographic directions ⟨100⟩, ⟨110⟩, and ⟨111⟩. The measured resistivity was .49 Ω-cm for the ⟨100⟩ sample, .68 Ω-cm for the ⟨110⟩ sample, and .50 Ω-cm for the ⟨111⟩ sample. The samples were then diffused at about 1100 °C in an induction heated vacuum furnace for 15 to 60 minutes. The tantalum bucket enclosing the wafers is prebaked at about 1700 °C to get rid of electrically active impurities. A diffusion grade phosphorous nitride was used as a donor source. The contamination background of this diffusion system is less than $10^{13}/cm^3$ added impurities. The time and the temperature were chosen to produce linearly graded junction impurity profiles. After diffusion some of these wafers were thinned to a thickness of about one mil so that hole and electron injection in the junction could be accomplished from opposite sides of the wafer.

2. Diode Profiling

The electric field profile of the junctions is obtained from capacitance measurements as a function of reverse bias. The data for a ⟨110⟩ diode is shown in Fig. 1 where it is seen that the inverse cube of the capacitance is a linear function of the bias out to breakdown. This linearly graded profile allows a more accurate determination of the maximum field in the junction than an asymmetric step junction. The reason is that in the step junction free carrier spillage from the heavily doped side significantly affects the maximum junction field. Thus for a linearly graded junction the simple Schottky approximation can be used to accurately determine the electric field. The following constants were determined for the junction of Fig. 1:

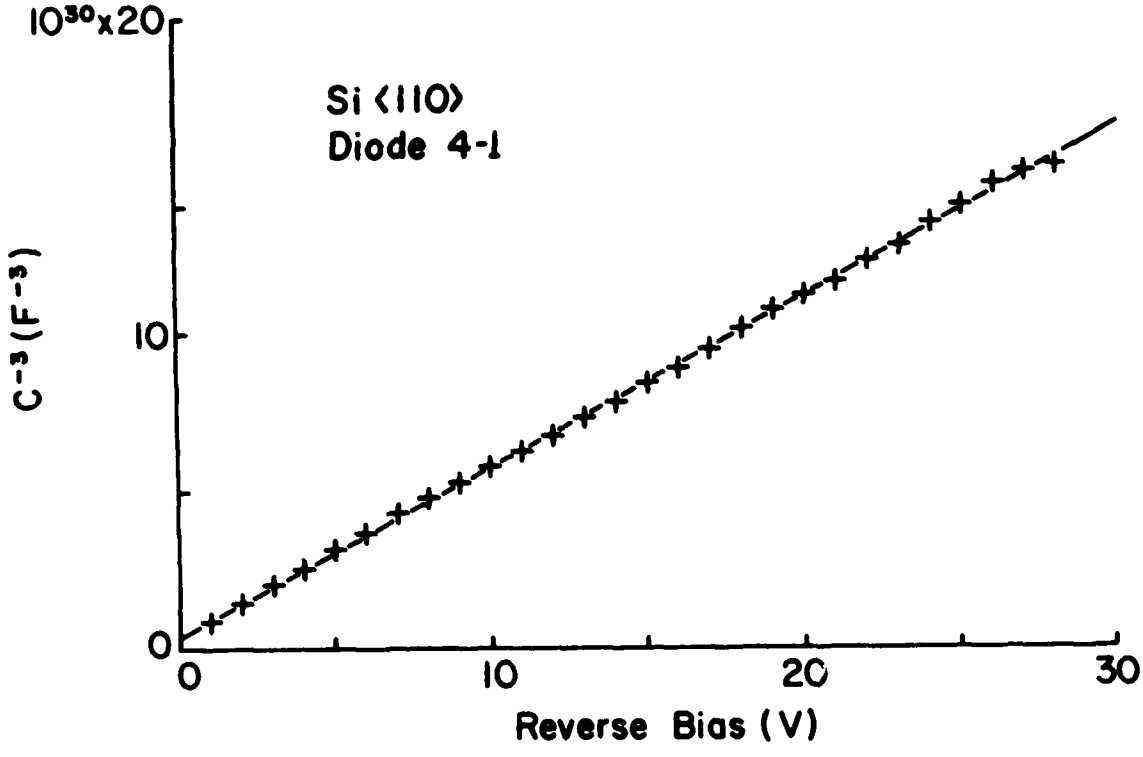

Figure 1. Diode capacitance data in the ⟨110⟩ direction.

$$\text{Area} = 4.2 \times 10^{-3} \text{ cm}^2 \quad ,$$

$$\frac{dN}{dx} = 1.73 \times 10^{21} \text{ cm}^{-4} \quad ,$$

$$V_{bi} = 0.7 \text{ Volts} \quad ,$$

$$\mathcal{E}_m = 4.2 \times 10^4 \, (V + V_{bi})^{2/3} \quad . \qquad (1)$$

The capacitance data for the ⟨100⟩ oriented diode is shown in Fig. 2. This data shows some curvature which is a consequence of the fact that the diffusion time was not long enough. The phosphorous distribution has roughly an exponential distribution into a uniform background of about $4.0 \times 10^{16}/\text{cm}^3$ acceptor concentration. The electric field near the maximum still has a parabolic shape, but the electric field dependence on the voltage is altered significantly near breakdown. The solid line in Fig. 2 shows the fit obtained by assuming an exponential diffused impurity gradient and a uniform background of acceptors,

$$N(x) = N_o(\exp(-x/L) - 1) \quad . \qquad (2)$$

Using this impurity distribution one can derive the following expressions for the electric field and the total junction potential:

$$\mathcal{E}_m = \frac{qN_oL}{\epsilon}\left[\frac{\omega}{e^{\omega}-1} - \ln\left(\frac{\omega}{e^{\omega}-1}\right) - 1\right], \qquad (3)$$

$$(V + V_{bi}) = \frac{qN_oL^2}{\epsilon}\,\omega\left[(\omega/2)\coth(\omega/2) - 1\right] \qquad (4)$$

where $\omega = w/L$, and w is the junction depletion width. The parameters of the fit to the data shown in Fig. 2 are:

$$\text{Area} = 1.7 \times 10^{-3} \text{ cm}^2 \quad ,$$

$$N_o = 4.1 \times 10^{16} \text{ cm}^4 \quad ,$$

$$L = 1.28 \times 10^{-5} \text{ cm} \quad ,$$

$$V_{bi} = 0.6 \text{ Volts} \quad .$$

Note that the background doping agrees well with that deter-

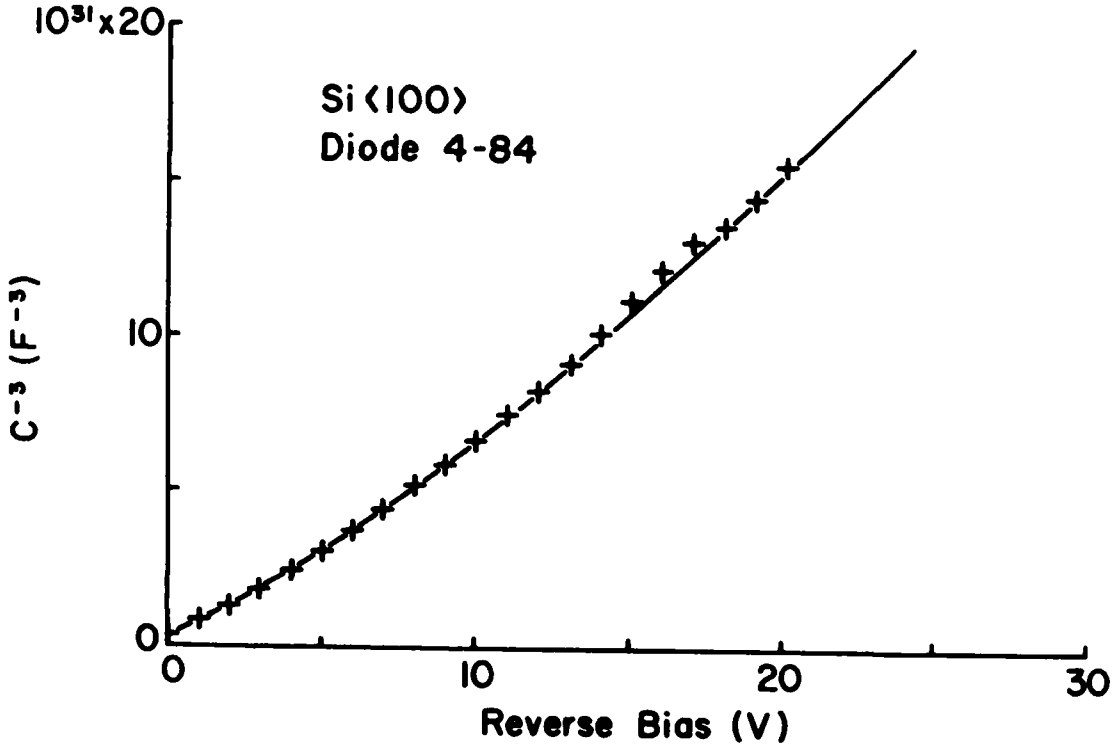

Figure 2. Diode capacitance data in the ⟨100⟩ direction.

mined from resistivity measurements before diffusion.

Capacity data for the ⟨111⟩ direction is not presented because multiplication data were directly compared with calculated multiplication using previously published ionization rates.[2] In addition, all of the parameters given above for the ⟨100⟩ and the ⟨110⟩ have an error tolerance of about 5%.

3. Photomultiplication Measurements

The electron and hole multiplication data for the ⟨110⟩ and the ⟨100⟩ directions, which are shown in Fig. 3, were obtained using two different techniques. To obtain pure electron and hole excitation of the avalanche a ⟨110⟩ oriented wafer was thinned to a thickness of slightly less than 25 μm, and non-penetrating radiation was used to illuminate the diode from opposite sides of the junction. The multiplication data obtained this way was compared with that obtained by using non-penetrating radiation (435.8 nm interference filter) from the n-side for hole excitation and using a GaAs filter to obtain penetrating radiation, again from the n-side, to obtain the electron excitation. This second technique relies on the fact that only a small number of holes will be generated in the diffused layer of about 1 micron thickness while electrons are collected over a distance of some 30 microns at least in the p-type substrate when penetrating radiation is used. Both techniques gave multiplication data for electrons and holes that agreed to within about 5%, so the simpler second technique was used to obtain the data on the ⟨100⟩ sample.

For comparison, Fig. 4 shows calculated electron and hole multiplication in the ⟨111⟩ direction for a breakdown voltage close to that of the ⟨110⟩ data. Perhaps the best way to illustrate the differences between the three crystal directions is to plot the multiplication versus the normalized

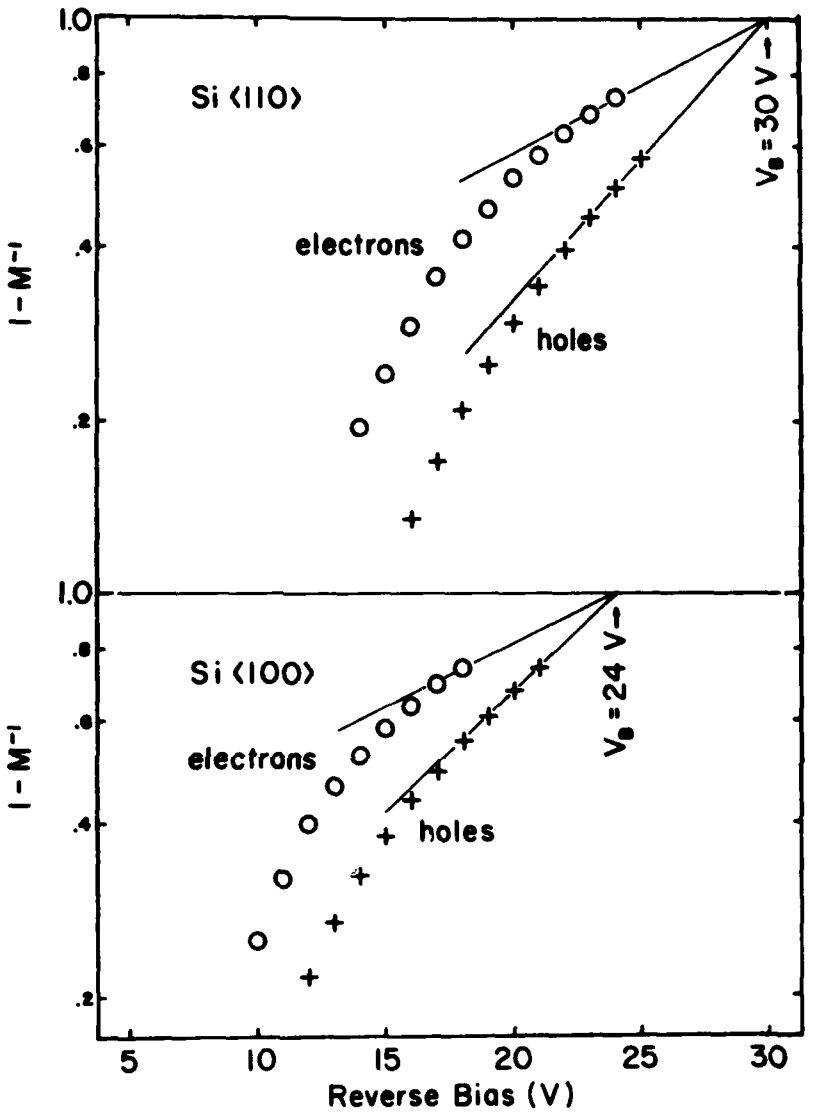

Figure 3. Multiplication data for ⟨110⟩ and ⟨100⟩ directions.

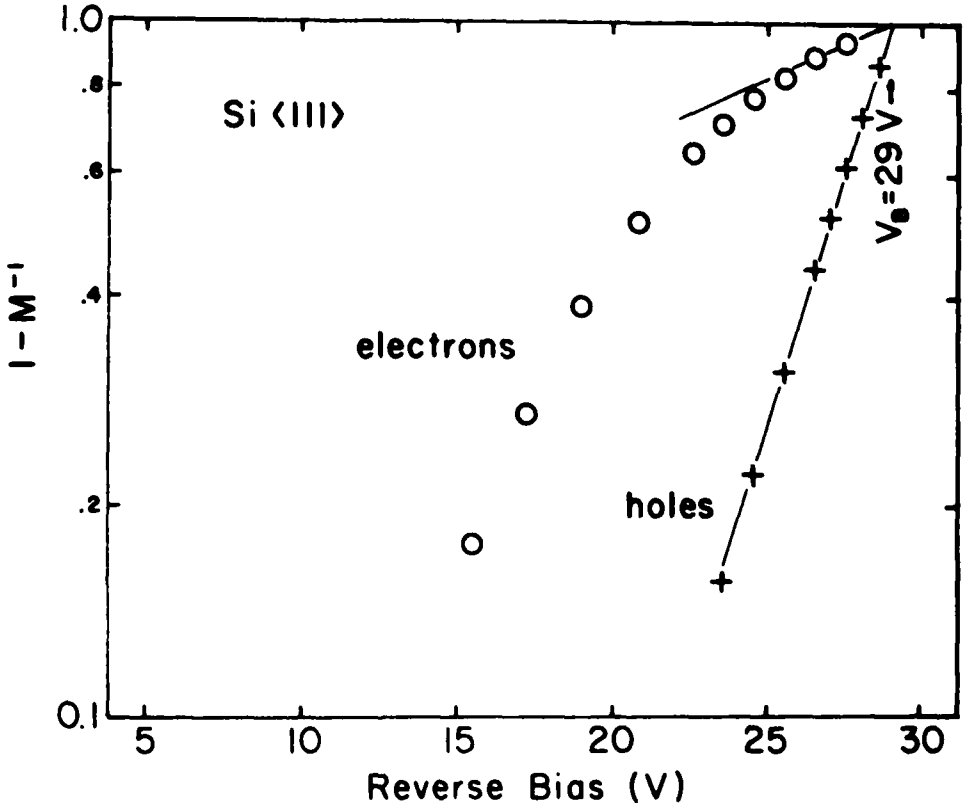

Figure 4. Multiplication data for the ⟨111⟩ direction.

voltage as is shown in Fig. 5. Here the highest multiplication and the smallest ratio of electron and hole multiplication is obtained in the ⟨100⟩ direction. In the ⟨110⟩ direction the multiplication is somewhat less and the ratio of electron to hole multiplication is slightly larger. In the ⟨111⟩ direction the electron multiplication is seen to be slightly smaller than the hole multiplication in the ⟨100⟩ direction while the hole multiplication is very much lower. This data implies that the lowest threshold ionization energy should be found in the ⟨100⟩ direction, an intermediate threshold for the ⟨110⟩ direction while the highest threshold should be found for the ⟨111⟩ direction. The implication of this data is thus at variance with the thresholds calculated by Anderson and Crowell except for the electron threshold in the ⟨100⟩ direction. The last section will consider non-colinear momentum constructions that can account for the observed multiplication data.

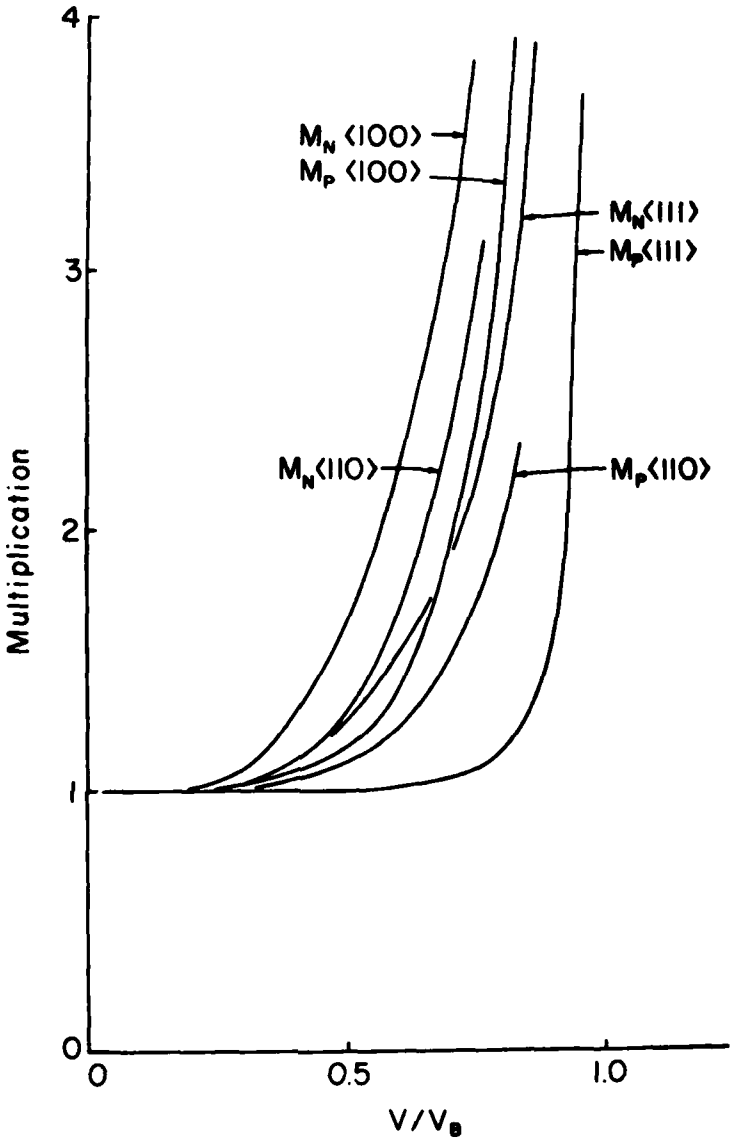

Figure 5. Multiplication data normalized to breakdown voltage.

SECTION III
IONIZATION RATES

For the linearly graded junctions we are considering the integral equations relating the ionization rates to the multiplication data are given by[2]

$$\frac{2}{w}\,\mathcal{E}_m^{\frac{1}{2}}\left[1-\frac{1}{M_n}\right]\left(\frac{M_n}{M_p}\right)^{\frac{1}{2}}=\int_0^{\mathcal{E}_m}\alpha\,\frac{d\mathcal{E}}{(\mathcal{E}_m-\mathcal{E})^{\frac{1}{2}}}\quad,\tag{5}$$

$$\frac{2}{w}\,\mathcal{E}_m^{\frac{1}{2}}\left[1-\frac{1}{M_p}\right]\left(\frac{M_p}{M_n}\right)^{\frac{1}{2}}=\int_0^{\mathcal{E}_m}\beta\,\frac{d\mathcal{E}}{(\mathcal{E}_m-\mathcal{E})^{\frac{1}{2}}}\quad.\tag{6}$$

These integrals are special cases of Abel's integral equation[3] and the solutions to Eqs. (5) and (6) can be written in the following form which is suitable for numerical evaluation:

$$\alpha(\mathcal{E}_m)=\frac{4\mathcal{E}_m}{\pi}\int_0^1 ds(1-s^2)^{\frac{1}{2}}\,\frac{d}{dV_s}\left[\left(1-\frac{1}{M_n}\right)\left(\frac{M_n}{M_p}\right)^{\frac{1}{2}}\right],\tag{7}$$

$$\beta(\mathcal{E}_m)=\frac{4\mathcal{E}_m}{\pi}\int_0^1 ds(1-s^2)^{\frac{1}{2}}\,\frac{d}{dV_s}\left[\left(1-\frac{1}{M_p}\right)\left(\frac{M_p}{M_n}\right)^{\frac{1}{2}}\right],\tag{8}$$

where $\mathcal{E}=\mathcal{E}_m(1-s^2)$, and the voltage derivative of the function of the multiplication is evaluated at the voltage V_s corresponding to a maximum electric field in the junction of $\mathcal{E}_s=\mathcal{E}_m(1-s^2)$.

The multiplication data shown in Fig. 3 has been used to evaluate Eqs. (7) and (8). It has been noted that the profile of the ⟨100⟩ sample is not quite a linearly graded junction, but it has been estimated that the slight asymmetry of the electric field distribution in the region where the ionization rates are appreciable should not change the result

obtained by assuming a linear gradient by more than 5%. The calculated ionization rates are plotted in Fig. 6. For comparison the previously published rates for the ⟨111⟩ direction[2] are shown in Fig. 7. At the present time it is not clear why the slope of the ionization rates gets progressively more negative as one goes from the ⟨100⟩ to ⟨110⟩ to the ⟨111⟩ direction.

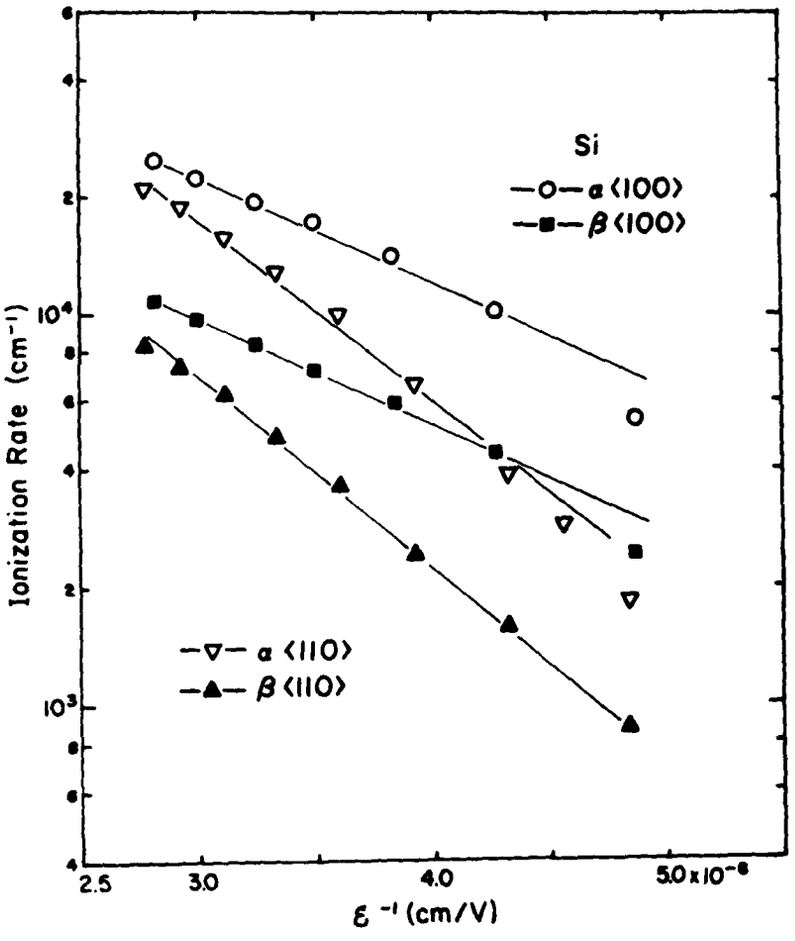

Figure 6. Ionization rates for ⟨100⟩ and ⟨110⟩ directions.

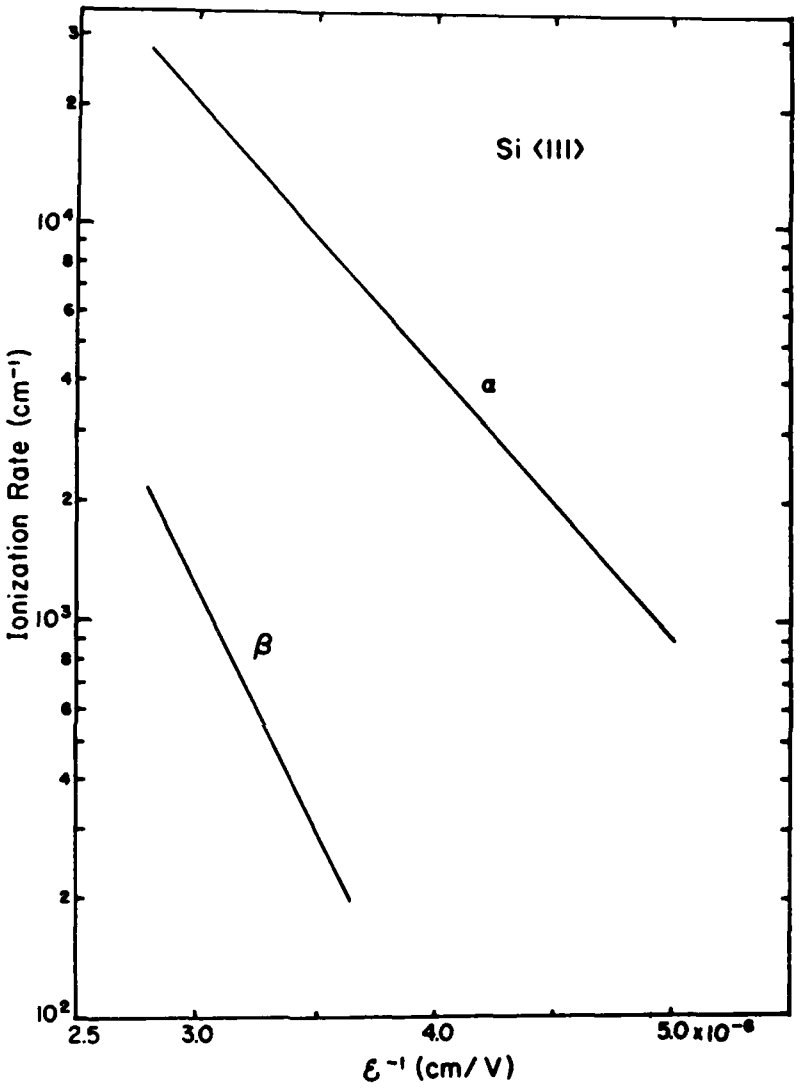

Figure 7. Ionization rates in the ⟨111⟩ direction.

SECTION IV

IONIZATION THRESHOLD ENERGIES

1. Old Threshold Estimates

The most complete estimate of the ionization threshold energies was carried out by Anderson and Crowell[1] who proceeded from the pseudopotential calculations of Chelikowsky and Cohen,[3] which are shown in Fig. 8 along with the zone scheme for silicon which is shown in Fig. 9 for reference. In working out their graphical solutions they assumed that the wave vector of the initiating particle, the velocities of the three particles after the collision, and the wave vector from the zone center to the conduction band minimum were all colinear. Figure 10 shows the ⟨100⟩ trajectory (X - Γ - X), and the ⟨110⟩ trajectory (X - K - Γ - K - X). Figure 11 shows the trajectory in the ⟨111⟩ direction (L - Γ - L). Their lowest threshold energy is for electrons in the ⟨100⟩ direction, 1.1 eV. The threshold energy for holes in the same direction was 1.8 eV. In the ⟨110⟩ direction they found a threshold energy of 3.1 eV for electrons and a hole energy of 1.8 eV. Finally in the ⟨111⟩ direction they obtained threshold energies of 3.1 eV for electrons and 2.9 eV for holes. As noted before these threshold energies do not correspond to the observed multiplication.

In the course of this work it was realized that other trajectories should be considered. Additional trajectories were considered that were parallel to the principal crystal directions, but passed through the conduction band minimum along the ⟨100⟩ axes. The band energies along these trajectories were plotted out but the estimated threshold energies did not even qualitatively agree with the observed data.

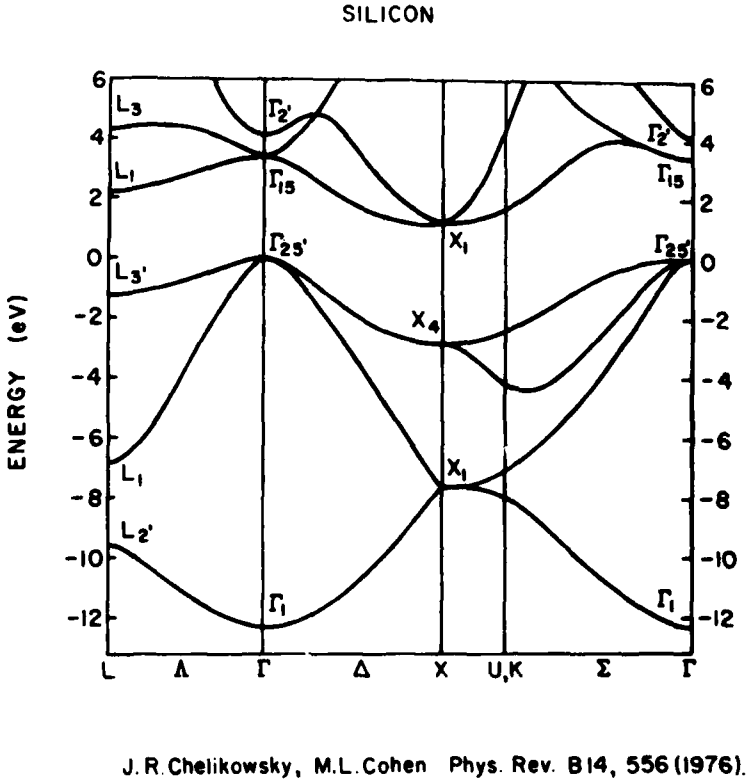

Figure 8. Calculated band structure of silicon.

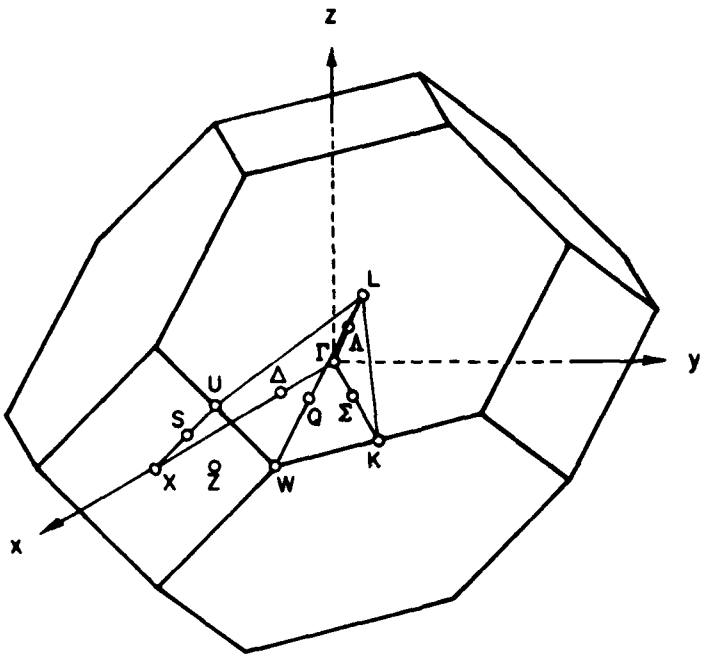

Figure 9. Brillouin zone of silicon.

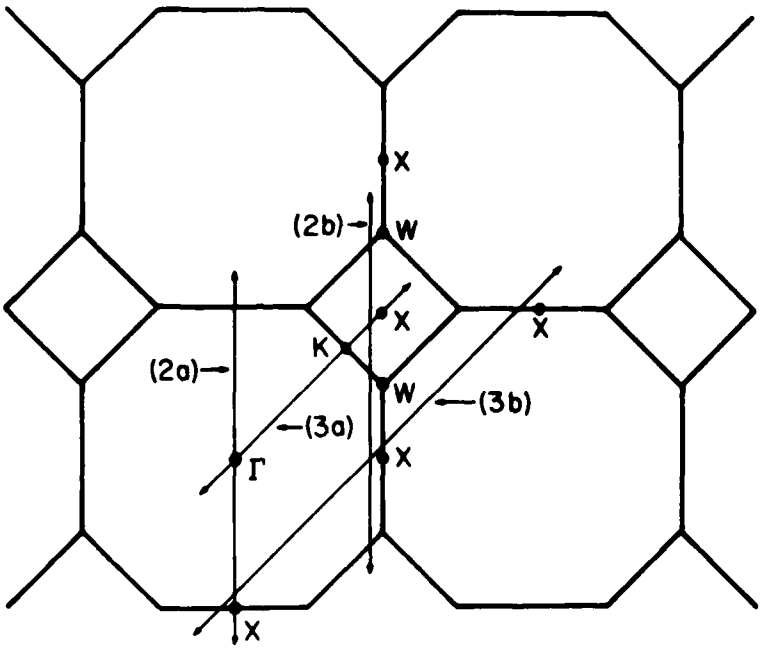

Figure 10. Particle trajectories through Brillouin zone in ⟨110⟩ and ⟨100⟩ directions passing through the zone center and through the conduction band minimum.

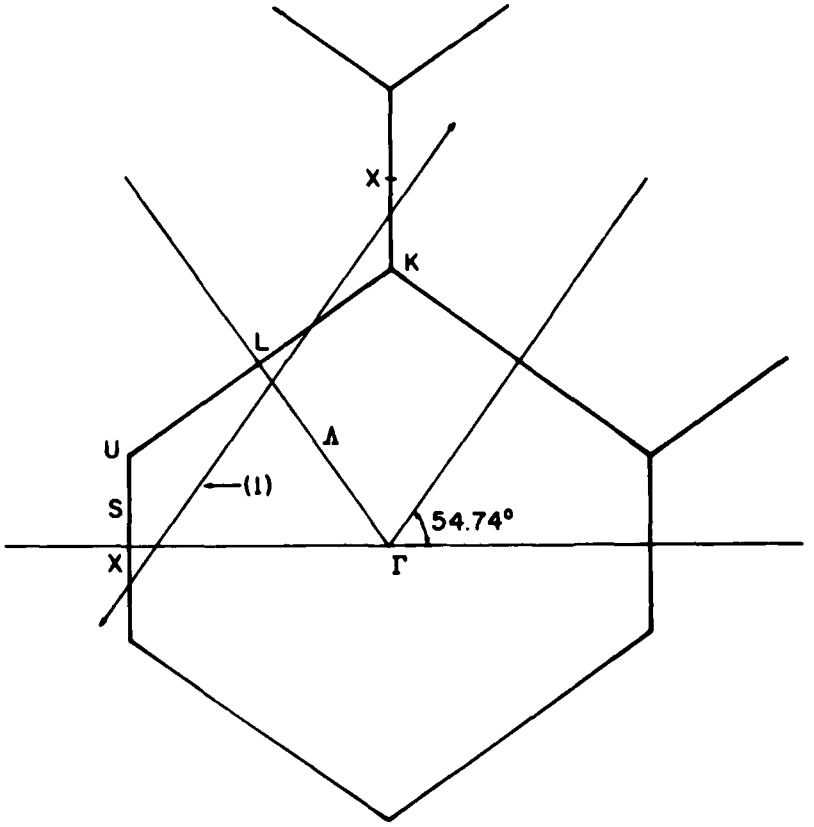

Figure 11. Particle trajectories through the Brillouin zone in the ⟨111⟩ direction passing through the zone center and through the conduction band minimum.

These trajectories, however, also made the assumption that all the vectors were colinear. It was eventually realized that the wave vector of the initial particle need not be colinear with the final wave vectors nor with the wave vector from the center of the zone to the conduction band minimum. Since the geometry can be quite complex, consider the situation illustrated in Fig. 12. Here the k_x-axis is coincident with the ⟨100⟩ direction and the k_y-axis intersects the ⟨111⟩ direction. We also consider an electric field parallel to the ⟨111⟩ direction, making the angle psi equal to 54.7 degrees. The initial velocity will not be parallel to the field, but will make an angle θ with the k_x-axis. Since the secondary hole is in a nearly spherical band its velocity and wave vector are essentially parallel. Then we note that the extremum of minimum threshold energy under the condition of conservation of crystal momentum requires that all three final velocities be colinear. Thus if the hole is in a spherical band while the two electrons are in a band with ellipsoidal energy surfaces, the wave vectors will not in general be parallel.

2. New Processes for Determining Threshold Energies

We have posed a difficult problem which has not been solved, but there is an approximate solution which qualitatively agrees with the observed multiplication data. The approximation we wish to consider is the following: at the minimum threshold energy the particle energies after the collision should be quite small, thus only a small error should be incurred if one assumes the wave vectors and the velocities of the final particles to be parallel. The wave vector from the zone center to the conduction band minimum, however, is large and we still allow this vector to be non-colinear. We also will assume that the band energies are parabolic in the plane containing the electric field and passing through the

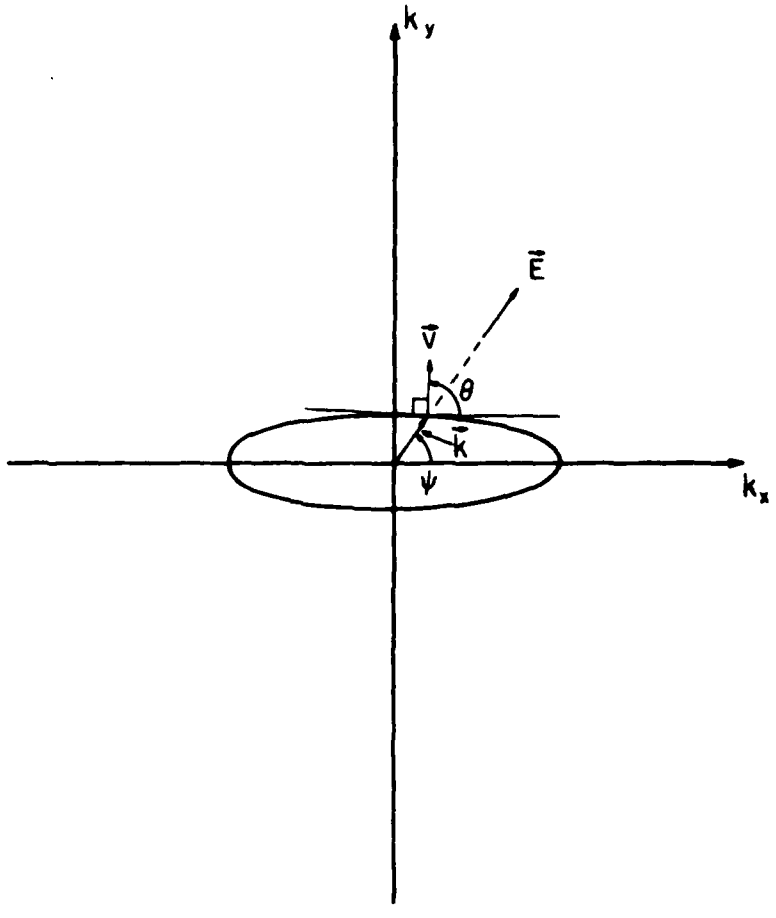

Figure 12. Non-colinear construction for determining the ionization threshold energy.

conduction band minimum or the valence band maximum.

The assumption of parabolic bands allows us to write the energies of the initial and final three particles,

$$E_{2'} = \hbar^2(\vec{k}_{2'} - \vec{k}_o)^2/2m_e \quad , \qquad (9)$$

$$E_1 = \hbar^2(\vec{k}_1 - \vec{k}_o)^2/2m_e \quad , \qquad (10)$$

$$E_2 = \hbar^2(\vec{k}_2 - \vec{k}_o)^2/2m_e \quad , \qquad (11)$$

$$E_{1'} = \hbar^2(\vec{k}_{1'})^2/2m_h \quad , \qquad (12)$$

where the subscript 2' denotes the initial electron (in this case), 1 and 2 denote the secondary electron and the initial electron after collision, and 1' denotes the secondary hole. Conservation of energy and crystal momentum give the following relations,

$$E_{2'} = E_1 + E_2 + E_{1'} + E_g \quad , \qquad (13)$$

$$\vec{k}_{2'} = \vec{k}_1 + \vec{k}_2 + \vec{k}_{1'} \quad , \qquad (14)$$

where E_g denotes the energy gap and phonon cooperation is neglected. The minimum threshold energy is obtained from the variational equation

$$\delta\left\{E_{2'} + \vec{\beta}\cdot\vec{k}_{2'}\right\} = 0 \quad , \qquad (15)$$

where the vector $\vec{\beta}$ is a Lagrange multiplier. The result of Eq. (15) is that all the final wave vectors are colinear,

$$\vec{k}_1 - \vec{k}_o = \vec{k}_2 - \vec{k}_o = (m_e/m_h)\,\vec{k}_{1'} \quad , \qquad (16)$$

and in the more general case it would be the velocities which would be colinear. The non-colinear part of the problem, $\vec{k}_o$, is not parallel, in general, to the wave vectors $\vec{k}_{2'}$, $\vec{k}_1$, $\vec{k}_2$, or $\vec{k}_{1'}$. By a somewhat lengthy manipulation of Eqs. (13),

(14) and (15) we can obtain an expression for $E_{2'}$ in terms of the band gap energy, the displacement of the conduction band minimum from the zone center, and the ratio of the hole to electron effective mass,

$$\frac{E_{2'}}{E_g} = \frac{2+\mu}{1+\mu} + \frac{1+\mu+2\cos^2\theta}{(1+\mu)^2}\, x - \frac{2\cos\theta}{(1+\mu)^2}\left\{x\left[x(1+\mu+\cos^2\theta)+(2+\mu)(1+\mu)\right]\right\}^{\frac{1}{2}}, \quad (17)$$

where θ is the angle between the wave vectors $\vec{k}_{2'}$ and $\vec{k}_o$, μ is the mass ratio m_h/m_e, and $x = E_o/E_g$, where $E_o = \hbar^2 k_o^2/2m_e$. It is immediately apparent that Eq. (17) reduces to a familiar result for a direct gap semiconductor (i.e. $k_o = 0$)

$$\frac{E_{2'}}{E_g} = \frac{2+\mu}{1+\mu} \quad . \quad (18)$$

Another case of immediate interest is the ⟨100⟩ direction in silicon where $\theta = 0$ and all the vectors are colinear

$$\frac{E_{2'}}{E_g} = \frac{2+\mu}{1+\mu} + \frac{3+\mu}{(1+\mu)^2}\, x - \frac{2}{(1+\mu)^2}\left[x(x+1+\mu)(2+\mu)\right]^{\frac{1}{2}} . \quad (19)$$

Equation (19) contains the surprising result that for $x = 1$ the threshold energy is exactly the band gap energy whereas for $x = 0$ we get the classical result of Eq. (18). One would expect that displacing the conduction band minimum away from the zone center would increase rather than decrease the threshold energy. One further point is to be made concerning Eq.(17) and that is that one can obtain the case of a hole being the energetic initial particle by simply inverting the mass ratio μ. This fact is made more transparent by translating the origin in k-space to the conduction band minimum when an energetic hole is the initial particle.

We now apply Eq. (17) to the three crystalline directions in silicon by calculating the effective mass in a given orientation with respect to the energy ellipsoids from the equation

$$E = \frac{\hbar^2 k_x^2}{2m_l} + \frac{\hbar^2 k_y^2}{2m_t} = \frac{\hbar^2 k^2}{2m_e^*} \quad , \qquad (20)$$

and the value of m_e^* is also used to evaluate the expression for x

$$x = \frac{E_o}{E_g} = \frac{\hbar^2 k_o^2}{2m_e^*} \cdot \frac{1}{E_g} \quad , \qquad (21)$$

and where k_o is taken to be 0.9 times the distance to the band edge in the ⟨100⟩ direction. Using the effective masses $m_l = (.98)m_o$, $m_t = (.19)m_o$, and $m_h = (.52)m_o$ we have calculated the threshold energies of electrons and holes for the three directions and listed them in Table 1.

It is clear from the calculated thresholds listed in Table I for the three crystal orientations that they are consistent with the experimental measurements. In fact the agreement is sufficiently encouraging to warrant carrying out the complete calculation where the velocities and wave vectors are not assumed to be colinear.

TABLE I

CALCULATED THRESHOLD ENERGIES IN SILICON

Orien.	0 degrees	x	μ	E_2/E_g elec.	E_2/E_g holes
⟨100⟩	0.	.98	.53	1.00	1.00
	90.	5.03	2.74	2.62	5.42
⟨110⟩	45.	3.01	1.63	1.41	1.58
	90.	5.03	2.74	2.62	5.42
⟨111⟩	54.74	3.68	2.00	1.62	2.02

REFERENCES

1. C. L. Anderson and C. R. Crowell "Threshold Energies for Electron-Hole Pair Production by Impact Ionization in Semiconductors," Phys. Rev. B 5, No. 6, pp. 2267-2272, 15 Mar 1972.
2. C. A. Lee, R. A. Logan, R. L. Batdorf, J. J. Kleimack, and W. Wiegmann "Ionization Rates of Holes and Electrons in Silicon," Phys. Rev. 134, No. 3A, pp A761-A773, 4 May 1964.
3. J. R. Chelikowsky and M. L. Cohen "Nonlocal Pseudopotential Calculations for the Electronic Structure of Eleven Diamond and Zinc-Blende Semiconductors," Phys. Rev. B 14, No. 2, pp 556-582, 15 Jul 1976.

MISSION
of
Rome Air Development Center

RADC plans and executes research, development, test and selected acquisition programs in support of Command, Control Communications and Intelligence (C^3I) activities. Technical and engineering support within areas of technical competence is provided to ESD Program Offices (POs) and other ESD elements. The principal technical mission areas are communications, electromagnetic guidance and control, surveillance of ground and aerospace objects, intelligence data collection and handling, information system technology, ionospheric propagation, solid state sciences, microwave physics and electronic reliability, maintainability and compatibility.

Printed by
United States Air Force
Hanscom AFB, Mass. 01731


DATE
ILME